# Totally Asymmetric Simple Exclusion Process on Networks

Izaak Neri,[1,2] Norbert Kern,[1,2] and Andrea Parmeggiani[3,4]

[1]*Université Montpellier 2, Laboratoire Charles Coulomb UMR 5221, F-34095, Montpellier, France*
[2]*CNRS, Laboratoire Charles Coulomb UMR 5221, F-34095, Montpellier, France*
[3]*Université Montpellier 2, Laboratoire DIMNP UMR 5235, F-34095, Montpellier, France*
[4]*CNRS, Laboratoire DIMNP UMR 5235, F-34095, Montpellier, France*

(Received 6 May 2011; revised manuscript received 21 June 2011; published 5 August 2011)

We study the totally asymmetric simple exclusion process (TASEP) on complex networks, as a paradigmatic model for transport subject to excluded volume interactions. Building on TASEP phenomenology on a single segment and borrowing ideas from random networks we investigate the effect of connectivity on transport. In particular, we argue that the presence of disorder in the topology of vertices crucially modifies the transport features of a network: irregular networks involve homogeneous segments and have a bimodal distribution of edge densities, whereas regular networks are dominated by shocks leading to a unimodal density distribution. The proposed numerical approach of solving for mean-field transport on networks provides a general framework for studying TASEP on large networks, and is expected to generalize to other transport processes.

DOI: 10.1103/PhysRevLett.107.068702 PACS numbers: 89.75.Hc, 02.50.−r, 05.60.Cd, 64.60.−i

Delivering matter, energy, or information is a crucial requirement for the functioning of any complex system, ranging from the subcellular level of biological organisms to globe-spanning man-made structures. Transport is often organized along linelike pathways, which are in turn interconnected to form a network structure. In this perspective, diffusion along networks has been studied extensively (see, e.g., [1,2]). On the other hand, interactions play a fundamental role in the transport properties of many systems: intracellular traffic of molecular motors on the cytoskeleton, pedestrian traffic on an ensemble of paths, and traffic of information packages on the Internet are but a few prominent examples where they lead to emergent collective phenomena, such as the appearance of jams.

The totally asymmetric simple exclusion process (TASEP) is a paradigmatic model for one-dimensional nonequilibrium transport subject to excluded volume interactions: entities (''particles'') hop in a given direction, but cannot occupy the same place [3]. TASEP was initially introduced as a model for the kinetics of RNA polymerization by ribosomes [4], but has since then received much general interest, including from fundamental statistical physics [5] and mathematics [6]. Numerous generalizations have been developed and applied to various areas, such as the collective motion of motor proteins along cytoskeletal filaments, vehicular traffic, etc. [7,8].

The collective behavior of exclusive transport on a network, however, is not well understood at this stage. A body of numerical work on TASEP-like models on networks, often with complex details, exists in the context of traffic [8], but less so on biological transport [9]. In terms of a paradigmatic analysis based on TASEP, knowledge is still limited to either simple topologies with at most two junctions [10,11], or involves structureless links, e.g., in treelike networks [12].

In this Letter we address the question of how the topology of a network affects its TASEP transport characteristics. Combining concepts from the area of complex networks [1] with mean-field (MF) methods for TASEP in the presence of junctions [11] we construct the global behavior from that of single segments. This allows us to rationalize many features of transport on large-scale random networks in terms of theoretical arguments, and furthermore leads to an algorithm to solve for MF TASEP transport on a large-scale network. In particular, we argue that irregularity, i.e., randomness in the vertex degrees, strongly modifies the transport properties of a network.

*TASEP on a network.*—We generalize the TASEP transport rules [3,4] to a closed network of $N_S$ directed segments and $N_V$ vertices or junctions (see Fig. 1 for an illustration). The segments consist of $L$ sites along which particles perform unidirectional random sequential hops subject to hard-core on-site exclusion. At the junctions, particles from $k_v^{\text{in}}$ incoming segments compete for occupying the same vertex site $v$, while a particle can leave the junction through one of $k_v^{\text{out}}$ outgoing segments with equal probability. We write $\rho_v$ for the average occupancy of a vertex $v$ with $0 \leq \rho_v \leq 1$. Particle number conservation in the junction $v$ reads

$$\frac{\partial \rho_v}{\partial t} = \sum_{v' \to v} J_{(v',v)} - \sum_{v'' \leftarrow v} J_{(v,v'')}. \tag{1}$$

The sums run over vertices $v'$ identifying incoming segments $(v', v)$ and over $v''$ for outgoing segments $(v, v'')$.

We briefly review the behavior of an isolated segment linked to reservoirs, which we will build on. Its average density $\rho$ and current $J$ are known to be homogeneous, provided that segments are at least of moderate size, such

 

that boundary effects remain small. Both are set by the entry rate $\alpha$ and exit rate $\beta$ [13]:

$$\rho(\alpha,\beta)=\begin{cases}\alpha & \alpha\le\beta,\ \alpha<1/2 \quad \text{(LD)}\\ 1-\beta & \beta\le\alpha,\ \beta<1/2 \quad \text{(HD)}\\ 1/2 & \alpha,\beta\ge 1/2 \quad \text{(MC)}\end{cases} \tag{2}$$

with the current given by the current-density relation

$$J(\alpha,\beta)=\rho(\alpha,\beta)(1-\rho(\alpha,\beta)). \tag{3}$$

These three homogeneous phases are high density (HD), low density (LD), and maximal current (MC), but for $\alpha=\beta$ a nonhomogeneous shock phase (SP) arises, for which LD and HD regions coexist on the same segment, separated by a diffusing domain wall [14].

*Mean-field theory and algorithm.*—We extend the MF analysis of [11] to large-scale networks to establish an algorithm operating on the junction occupancies $\rho_v$ as the only variables. Using MF [13] we neglect correlations between neighboring sites. Then the entry (exit) rate $\alpha$ ($\beta$) for a segment are effective rates, which depend only on the occupancies of the adjacent vertices [11]:

$$\alpha=\rho_{v'}/k^{\text{out}}_{v'} \quad \text{and} \quad \beta=1-\rho_{v''}. \tag{4}$$

The entry rate $\alpha$ is reduced according to the out-degree $k^{\text{out}}_{v'}$, since particles on vertex $v'$ are distributed uniformly over all outgoing edges. Assuming homogeneous segments, the effective rates in (2) and (3) can be substituted into the continuity equation (1) to yield a closed set of $N_V$ equations in the vertex occupancies:

$$\frac{\partial\rho_v}{\partial t}=\sum_{v'\to v}J\left(\frac{\rho_{v'}}{k^{\text{out}}_{v'}},1-\rho_v\right)-\sum_{v''\leftarrow v}J\left(\frac{\rho_v}{k^{\text{out}}_{v}},1-\rho_{v''}\right), \tag{5}$$

where the sums run over all vertices $v'$ ($v''$) which are upstream (downstream) from $v$. The microscopic dynamics lack particle-hole symmetry at the junctions, as is reflected in Eq. (5) by the factor $1/k^{\text{out}}_{v'}$ in the entry rate.

Our numerical MF algorithm iteratively finds the stationary solution to (5), thereby achieving considerable computational advantage upon simulations since we only need to update the $N_V$ junction occupancies $\rho_v$. In the following we study transport on random networks as model systems, complementing MF solutions of Eqs. (5) by explicit simulations. Throughout, we exploit the fact that macroscopic observables are self-averaging on these ensembles, as we have verified by analyzing different network instances.

*Bethe networks.*—As an example of closed random graphs with regular topology we consider the directed Bethe network, drawn from the $c$-regular ensemble [15], in which all vertices have identical connectivity $c=k^{\text{in}}=k^{\text{out}}$. The undirected Bethe network is well known in statistical mechanics, for example of spin models on graphs [16]. Figure 2 shows the average segment current $J$ as a function of the overall density $\rho$. The standard result for the current $J(\rho)=\rho(1-\rho)$ is recovered for $c=1$, where the Bethe network reduces to a simple ring. As connectivity is increased, the overall current drops: this may appear counterintuitive, but reflects the fact that vertices progressively become bottlenecks and block the flow of particles. More precisely, the current parabola is truncated at intermediate densities by a plateaulike region, which widens but lowers with connectivity $c$. To interpret these results, we first give an explanation based on the phenomenology of TASEP on a line. To this end, we point out that an analytical solution to Eqs. (5) can be given for the Bethe network, since all $N_V$ equations become identical due to equal vertex connectivities. Therefore the solution requires identical occupancies $\rho_v$ for all vertices, from which segment currents and densities follow: all vertices, and therefore all segments, are equivalent. The transition from LD to HD appears when the effective rates (4) are equal ($\alpha=\beta$), i.e., at $\rho_v=c/(c+1)$. Using Eqs. (2)–(4) this leads to distinct regimes for the current, yielding the truncated parabola for the MF current-density relation:

$$J(\rho)=\begin{cases}\frac{c}{(c+1)^2} & \text{for } \rho^*<\rho<1-\rho^*,\\ \rho(1-\rho) & \text{otherwise,}\end{cases} \tag{6}$$

with LD phases (for $\rho<\rho^*$), and HD phases (for $\rho>1-\rho^*$), where $\rho^*=1/(c+1)$. The plateau can be

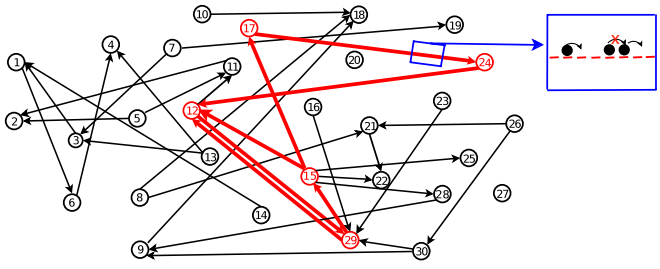

FIG. 1 (color online). An example of a Poissonian network of $M=30$ junctions with average connectivity $c=1$ and its strongly connected component (bold). Every segment consists of $L$ sites on which particles undergo TASEP dynamics. At the junctions the particles choose one of $k^{\text{out}}_v$ outlets.

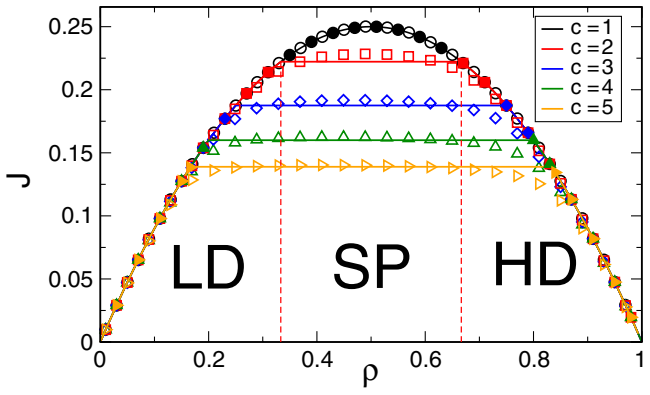


FIG. 2 (color online). The average segment current $J$ as a function of the overall density $\rho$ on a Bethe network of degree $c$ superposing numerical mean-field predictions (closed symbols), explicit simulations ($N_V=80$ junctions, $L=100$ sites per edge, open symbols), and a one-vertex analytical result Eq. (6) (solid lines). The dashed lines delimit the phases for $c=2$.

rationalized in terms of domain wall phenomenology [14], recalling that $\alpha = \beta$ indicates a SP with a diffusing domain wall between LD and HD zones which coexist on the same segment. Since both zones have complementary densities ($\rho_{\mathrm{LD}} = 1 - \rho_{\mathrm{HD}}$), the current is not affected as further particles are accommodated by growing the HD zones at the expense of the LD zones [14,17].

These MF arguments capture the essential transport features well, as is shown by the simulation data on Fig. 2 (which remains true for triangular and square lattices). Deviations from finite size simulations arise, however, on the current plateau (underestimated by MF) and close to the transitions (where particle-hole asymmetry increases with connectivity $c$). The numerical MF algorithm does not provide a solution on the plateau, since the assumption of homogeneous segments does not hold, but it otherwise reproduces the theoretical results with great precision. In summary, TASEP transport through a random Bethe network may be understood in terms of a single effective vertex, similar to the Ising model on a Bethe lattice [16].

*Poissonian networks.*—In order to explore the effect of irregularity, i.e., nonuniform vertex connectivity, we study TASEP on the Poissonian (Erdös-Rényi) ensemble [15]: any two vertices are connected with probability $c/N_V$, yielding an average connectivity $c$. In order to avoid artifacts we consider transport on the strongly connected component (SCC), in which each vertex can be reached from all other vertices (see Fig. 1 for an example). We find the SCC using an algorithm developed by Tarjan [18].

We first comment on the transport characteristic $J(\rho)$ of TASEP transport on Poisson networks. Figure 3 shows the current $J$ (averaged over all segments) as a function of density $\rho$, for various connectivities $c$. The MF results are in excellent agreement with simulations, thereby validating the MF algorithm for irregular networks. The comparison to Bethe networks with identical connectivities $c$ shows that both networks carry the same current $J(\rho)$ at very low and very high densities. However, they behave very differently at intermediate densities. We observe that (i) currents in Poissonian networks are significantly lower than in the corresponding Bethe networks, (ii) even on the MF level, the current $J(\rho)$ no longer possesses particle-hole symmetry ($\rho \leftrightarrow 1 - \rho$), and (iii) the density at which the highest current is achieved lies below half-filling, and progressively reduces with connectivity $c$. The most striking difference, however, is the absence of a plateau in $J(\rho)$ for the Poissonian network. In contrast to Bethe networks, this suggests that no SP segments involving domain walls arise over any extended density range.

A finer understanding is obtained by analyzing how transport is distributed across the individual segments of the network. Consider first the distribution of segment densities, shown for a connectivity $c = 10$ and an overall density $\rho = 0.3$, see Fig. 4(a). It is bimodal with peaks at very high and very low densities. We are therefore dealing with two subnetworks either in LD or HD phase, in

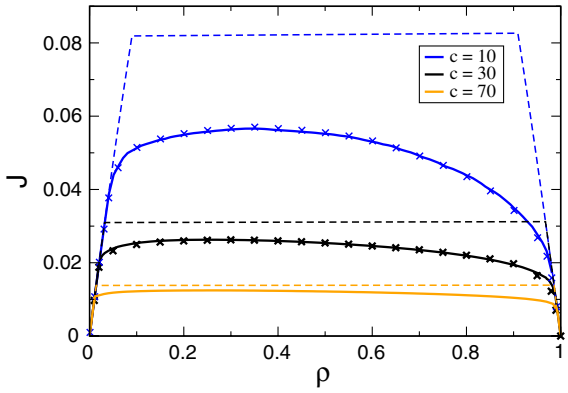


FIG. 3 (color online). The current-density relation of the strongly connected component of a Poissonian network of average connectivity $c$, $N_V = 200$ junctions. Simulations (markers, segments of $L = 100$ sites) coincide with mean field results for a given graph instance, resolving sample to sample fluctuations (of the order of the symbols size). For comparison, the Bethe result Eq. (6) is shown for the same $c$ (dotted lines).

contrast to the Bethe scenario where all segments are in a SP at indermediate densities. Interestingly, the distribution of the segment currents remains unimodal for Poisson networks, Fig. 4(b), thus putting a similar load on all segments.

The bimodal density distribution is also the key to understanding how the network adjusts to higher overall densities, by successively switching individual segments from LD to HD. The inset in Fig. 4(a), obtained for $\rho = 0.7$, shows that the typical densities of HD/LD segments are not significantly modified, whereas the proportion of the HD network grows at the expense of its LD counterpart as further particles are added. This is further documented by the fraction $n_{\mathrm{HD}}$ ($n_{\mathrm{LD}}$) of edges in HD (LD) phases, Fig. 4(c). For the Poissonian network $n_{\mathrm{HD}}$ is roughly equal to the overall density $\rho$, thereby confirming that the change from LD to HD in irregular networks occurs progressively. This linear behavior of $n_{\mathrm{HD}}$ is furthermore very robust with respect to variations of average connectivity $c$ (data not shown), implying that this picture remains valid for all connectivities $c$.

*Transport on highly connected networks.*—Significant insight into TASEP transport on general random networks can be gained from analyzing the (MF) high-connectivity limit. Ultimately all vertices constitute bottlenecks, taking their occupancy close to saturation. Therefore we expand the MF equations (5), posing $\rho_v = 1 - r_v/c$, with $r_v \sim \mathcal{O}(1)$ (see Supplemental Material [19])

$$W_S(\rho_s) = \sum_k \frac{p_{\mathrm{deg}}(k)k}{c} \int dr W_V(r)\delta(\rho_s - \rho_\pm), \qquad (7)$$

where $p_{\mathrm{deg}}(k)k/c$ represents the degree distribution of vertices when selecting a random segment. $W_V(r)$ is the distribution of $r$, which follows from the MF equations (5). The high (low) density value $\rho_+$ ($\rho_-$) are set by the vertex saturation parameter $r/c$ relative to the vertex degree $k$, as

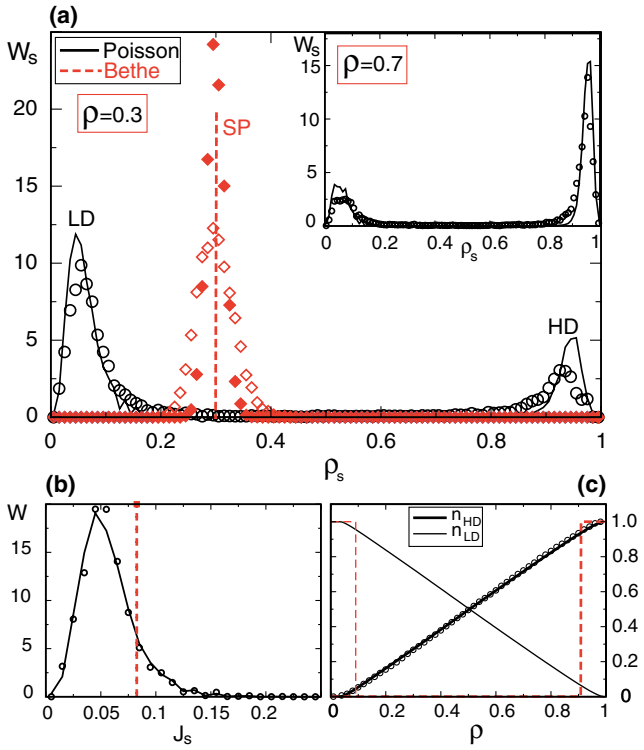


FIG. 4 (color online). Distribution of segment properties for networks of connectivity $c = 10$, comparing a Poisson network (black) to a Bethe network (dashed red). Symbols show simulation results, lines are mean-field predictions. (a) Distribution of segment densities $W_S(\rho_s)$ for an overall density $\rho = 0.3$ (inset: $\rho = 0.7$). Convergence of the density peak to a delta peak is very slow in simulations due to collective fluctuations in the shock phase, closed markers correspond to fourfold longer runs than open ones. (b) Distribution of segment currents $W(J_s)$ for $\rho = 0.3$. (c) Fraction of segments in high ($n_{\mathrm{HD}}$) and low ($n_{\mathrm{LD}}$) density segments as a function of the overall density $\rho$.

$$\rho_{\pm} = \begin{cases} \rho_{-} = 1/k & \text{if } r/c > 1/k, \\ \rho_{+} = 1 - r/c & \text{if } r/c < 1/k. \end{cases} \tag{8}$$

This shows that the bimodal distribution $W_S$ in the segment densities, with a fraction of segments in LD and a fraction in HD, is a general feature for complex irregular networks. This is particularly well illustrated in the strong connectivity limit $c \to \infty$, where $W_S(\rho_s)$ reduces to

$$W_S(\rho_s) = (1 - \rho)\delta(\rho_s) + \rho\delta(1 - \rho_s). \tag{9}$$

The weights of the $\delta$ functions explain the linear behavior of $n_{\mathrm{HD}}$, and our interpretation for Poissonian networks hence generalizes to general irregular random networks.

*Conclusions and outlook.*—TASEP transport on closed random networks has been shown to lead to very different scenarios for regular and irregular topologies. Despite the minimal character of TASEP, there may be direct implications: the presence of bimodality, which we have shown to be robust, in biological tracer experiments would make our findings directly useful for their interpretation. But our results also raise interesting questions, such as the interplay of biological transport and crowding, and their possible regulation by the cytoskeletal network.

An important result of our study is that MF arguments lead to very good predictions for the transport properties of closed networks, and provide a framework for their interpretation. Moreover, our numerical MF method gives access to system sizes currently beyond the reach of simulations. Generalizations of the approach to open random networks and other network topologies seem straightforward. In addition, we may expect it to generalize to other transport processes, as long as the behavior of individual segments is known and boundary controlled, i.e., determined by the occupancy of its junctions.

I. N. thanks Francesco Turci for many fruitful discussions. We thank A. C. Callan-Jones for a critical reading of the manuscript and acknowledge support from ANR-09-BLAN-0395-02 and from the University of Montpellier 2.

[1] A. Barrat, M. Barthélemy, and A. Vespignani, *Dynamical Processes on Complex Networks* (Cambridge Univ. Press, Cambridge, 2008).
[2] E. López *et al.*, Phys. Rev. Lett. **94**, 248701 (2005).
[3] G. M. Schütz, in *Phase Transitions and Critical Phenomena (19)*, edited by C. Domb and J. Lebowitz (Academic, London, 2000).
[4] J. T. MacDonald, J. H. Gibbs, and A. C. Pipkin, Biopolymers **6**, 1 (1968).
[5] *Nonequilibrium Statistical Mechanics in One Dimension*, edited by V. Privman (Cambridge University Press, Cambridge, U.K., 1997).
[6] T. M. Liggett, *Stochastic Interacting Systems: Contact, Voter and Exclusion Processes* (Springer, New York, 1999).
[7] E. Frey, A. Parmeggiani, and T. Franosch, Genome Inf. **15**, 46 (2004); D. Helbing, Rev. Mod. Phys. **73**, 1067 (2001).
[8] D. Chowdhury, A. Schadschneider, and K. Nishinari, Phys. Life Rev. **2**, 318 (2005); *Traffic and Granular Flow '07*, edited by C. Appert-Rolland *et al.* (Springer Verlag, Berlin, 2009).
[9] P. Greulich and L. Santen, Eur. Phys. J. E **32**, 191 (2010).
[10] J. Brankov, N. Pesheva, and N. Bunzarova, Phys. Rev. E **69**, 066128 (2004); E. Pronina and A. B. Kolomeisky, J. Stat. Mech. (2005) P07010; R. Wang *et al.*, Phys. Rev. E **77**, 051108 (2008).
[11] B. Embley, A. Parmeggiani, and N. Kern, Phys. Rev. E **80**, 041128 (2009).
[12] M. Basu and P. K. Mohanty, J. Stat. Mech. (2010) P10014; R. Stinchcombe, Physica (Amsterdam) **346A**, 1 (2005).
[13] B. Derrida, E. Domany, and D. Mukamel, J. Stat. Phys. **69**, 667 (1992).
[14] A. B. Kolomeisky *et al.*, J. Phys. A **31**, 6911 (1998).
[15] B. Bollobás, *Random Graphs* (Cambridge University Press, Cambridge, U.K., 2001).
[16] R. J. Baxter, in *Exactly Solved Models in Statistical Mechanics* (Academic Press, London, 1982), Chap. 4.
[17] B. Embley, A. Parmeggiani, and N. Kern, J. Phys. Condens. Matter **20**, 295213 (2008).
[18] R. E. Tarjan, SIAM J. Comput. **1**, 146 (1972).
[19] See Supplemental Material at http://link.aps.org/supplemental/10.1103/PhysRevLett.107.068702 for highly connected general networks.